Structures of the Dimeric and Monomeric Variants of Magainin Antimicrobial Peptides (MSI-78 and MSI-594) in Micelles and Bilayers, Determined by NMR Spectroscopy[†]

Fernando Porcelli,[‡,§] Bethany A. Buck-Koehntop,[‡] Sathiah Thennarasu,[∥] Ayyalusamy Ramamoorthy,*,[∥] and Gianluigi Veglia*,[‡]

Department of Chemistry, University of Minnesota, Minneapolis, Minnesota 55455, Department of Environmental Sciences, University of Tuscia, Viterbo, Italy, Department of Chemistry, University of Michigan, Ann Arbor, Michigan 48109-1055, and Biophysics Research Division, University of Michigan, Ann Arbor, Michigan 48109-1055

Received January 27, 2006; Revised Manuscript Received March 21, 2006

ABSTRACT: Magainins are antimicrobial peptides that selectively disrupt bacterial cell membranes. In an effort to determine the propensity for oligomerization of specific highly active magainin analogues in membrane mimetic systems, we studied the structures and lipid interactions of two synthetic variants of magainins (MSI-78 and MSI-594) originally designed by Genaera Corp. Using NMR experiments on these peptides solubilized in dodecylphosphocholine (DPC) micelles, we found that the first analogue, MSI-78, forms an antiparallel dimer with a "phenylalanine zipper" holding together two highly helical protomers, whereas the second analogue, MSI-594, whose phenylalanines 12 and 16 were changed into glycine and valine, respectively, does not dimerize under our experimental conditions. In addition, magic angle spinning solid-state NMR experiments carried out on multilamellar vesicles were used to corroborate the helical conformation of the peptides found in detergent micelles and support the existence of a more compact structure for MSI-78 and a pronounced conformational heterogeneity for MSI-594. Since magainin activity is modulated by oligomerization within the membrane bilayers, this study represents a step forward in understanding the role of self-association in determining magainin function.

Naturally occurring magainins (PGLa and magainin 2) are cationic peptides that have been shown to exhibit a broad spectrum of antimicrobial activities (*1*). Because of the growing drug-resistance threat, magainins have received an extraordinary amount of attention from many research groups, and several synthetic analogues have been synthesized and tested for clinical purposes (*1–4*). Among the different synthetic constructs, MSI-78 and MSI-594 were designed by Genaera Corp. as possible topical medicaments for bacterial infections. In particular, MSI-78 (known as plexiganon), a 22-residue magainin, was used in two phase III clinical trials for the treatment of diabetic foot ulcers (*5*). These trials show that MSI-78 is as effective as ofloxacin, a systemic drug orally administered for treating bacterial infections. In addition, in vitro assays show that MSI-78 is active toward ∼90% of the 411 aerobic bacteria isolated in

that study, with somewhat lower activity toward *Enterococcus faecalis* (*6*). Moreover, the combination of MSI-78 with other antibiotic drugs seems to be a possible new avenue against bacteria responsible for bloodstream infections in neutropenic patients (*7, 8*). On the other hand, MSI-594, which differs from MSI-78 in the primary sequence from the 10th residue and contains two additional C-terminal residues, has a pronounced activity against herpes simplex virus type 1 (HSV). While MSI-78 is thought to oligomerize into toroidal-type structures to permeate bacterial walls (*9, 10*), MSI-594 is unlikely to employ the same mechanism against viral envelops, whose function is not to maintain membrane potential and osmosis (*11*). Rather, MSI-594 may act through other membrane disruption mechanisms. To understand the biological activities of these two magainin compounds, it is imperative that we study the mechanism of self-aggregation and membrane interactions of these compounds.

While several biophysical studies characterized the monomeric form of magainin 2, Matsuzaki and co-workers emphasized the propensity of magainin 2 to form dimers (*12–14*), suggesting that the first step in understanding the function of magainins is to determine their relative tendency to oligomerize (*15*). In particular, studying disulfide-dimerized magainin 2 analogues in conjunction with F5Y, F16W magainin 2, these researchers concluded that dimerization is an important prelude to cell disruption and the monomer–dimer equilibria constitute a necessary step in the formation of pentameric pores (*16–18*). Another important aspect

* To whom correspondence should be addressed. A.R.: Biophysics Research Division, Department of Chemistry, University of Michigan, Ann Arbor, MI 48109-1055; telephone, (734) 647-6572; e-mail, ramamoor@umich.edu. G.V.: Department of Chemistry, University of Minnesota, 139 Smith Hall, 207 Pleasant St. S.E., Minneapolis, MN 55455; telephone, (612) 625-0758; fax, (612) 626-7541; e-mail, veglia@chem.umn.edu.
‡ University of Minnesota.
§ University of Tuscia.
∥ University of Michigan.

underlined by this study is the importance of choosing appropriate membrane mimicking systems for the structural and oligomerization studies of magainin 2 peptides. These researchers pointed out that while the studies in organic mixtures and detergent micelles produced monomeric structures, only lipid vesicles revealed the dimerization of magainin peptides. To determine the effects of membrane mimicking systems such as detergent micelles on the dimerization of magainin peptides, we elucidated the high-resolution structures of both MSI-78 and MSI-594 in dodecylphosphocholine micelles, a zwitterionic membrane mimetic system commonly used to study the structure of membrane proteins as well as antimicrobial peptides (*19−24*).

MATERIALS AND METHODS

Peptide Syntheses and NMR Sample Preparation. MSI-78 and MSI-594 were synthesized according to the procedure described by Maloy et al. (*25*). The NMR samples were prepared by dissolving the lyophilized peptides in an aqueous solution (10% ^2H_2O and 90% H_2O) containing 200 mM perdeuterated DPC (CIL) and 20 mM phosphate buffer at pH ∼4 at a final concentration of 1.6 mM.

Structure Determination. All solution NMR experiments were performed at 25 °C on a Varian Inova 600 MHz spectrometer equipped with an inverse detection triple-resonance probe. Complete assignments of the side chain and backbone resonances were obtained using 2D $^1H−^1H$ TOCSY (60 and 70 ms mixing times) and 2D $^1H−^1H$ NOESY (120 and 150 ms mixing times) experiments with 1024 complex points in the direct dimension and 256 points in the indirect dimension (*28, 29*). All two-dimensional (2D) spectra were processed by applying a sine-squared bell function shifted by 90° and zero-filling before Fourier transformation. Polynomial baseline correction was applied in the indirect dimensions. The 2D experiments were processed in a similar manner, with a linear prediction of 48−64 points in the ^{15}N dimension. All NMR spectra were processed using NMRPipe and analyzed using SPARKY (*26, 27*).

Magic Angle Spinning Solid-State NMR Experiments. A REDOR pulse sequence (*30*) was used to measure the ^{13}C isotropic chemical shift of MSI-78 that was labeled with $^{13}C'$-Ala$_{15}$ and ^{15}N-Phe$_{16}$ and MSI-594 that was labeled with $^{13}C'$-Ala$_{15}$ and ^{15}N-Val$_{16}$. To suppress the ^{13}C background signal from lipid molecules of multilamellar vesicles, we used REDOR-filtered experiments as described by Yang et al. (*31*). A 5 mm triple-resonance MAS probe tuned at the resonance frequency of ^{13}C at 100.8 MHz, of ^1H at 400.8 MHz, and of ^{15}N at 40.6 MHz was used at an 8 kHz spinning speed. A 1.5 ms ramp-cross polarization (*43*) was followed by a REDOR dephasing period and then direct ^{13}C detection with a recycle delay of 3 s. A single 55 kHz ^{13}C refocusing 180° pulse was placed at the center of the REDOR dephasing time, and a 74 kHz TPPM decoupling (*32*) was applied on the ^1H channel during both dephasing and detection. The ^{13}C and ^{15}N transmitters were set at 175 ppm (relative to tetramethylsilane) and 115 ppm (relative to liquid ammonia at 25 °C), respectively. For the S_1 (that is with 180° pulses in the ^{15}N channel) acquisition, a 45 kHz ^{15}N 180° pulse at the middle and end of each rotor period in the dephasing
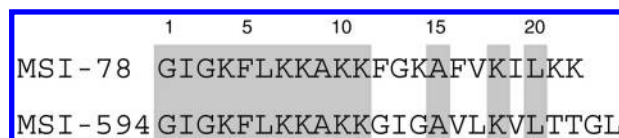

FIGURE 1: Primary sequences of MSI-78 and MSI-594. The shaded residues are identical in both sequences.

time was applied. Other details of the REDOR filtering experiment can be found elsewhere (*31*).

Structure Calculations. The MSI-594 structural ensemble was calculated starting from an extended structure using the simulated annealing protocol available in NIH-XPLOR to generate 100 conformers (initial temperature, T_i, of 5000 K with 6000 high-temperature steps, 3000 cooling steps, and a step size of 5 fs) (*33, 34*). A total of 160 NOEs, including 59 intra- and 101 interresidue NOEs, were classified as strong (1.8−2.8 Å), medium (1.8−3.5 Å), or weak (1.8−5.0 Å) and utilized as structural constraints. Structural refinement was carried out by systematically introducing Lennard-Jones potentials and van der Waals and electrostatic interactions using a T_i of 2000 K, with 10 000 cooling steps at a step size of 4 fs. Final refinement of the structure ensemble was calculated at a T_i of 500 K with 30 000 cooling steps at a step size of 1 fs.

The structural ensemble for dimeric MSI-78 was calculated starting from two helical protomers obtained from extended structures and folded using the simulated annealing procedure described above for MSI-594. The two protomers were then annealed to form a dimer gradually introducing interprotomer NOE distances using a temperature of 3000 K and a harmonic constant of 500 kcal/mol. After the first simulated annealing procedure, the structures were further refined starting from a temperature of 1000 K for 40 000 steps. The final refinement was carried out by introducing van der Waals and Ramachandran as well as electrostatic energy terms for a total of 40 000 steps of molecular dynamics. Note that to avoid a bias in our conformational search, we modeled the dimer without using the XPLOR symmetry function for the NOEs.

The 40 refined structures had no NOE violations of >0.4 Å, no bond violations of >0.05 Å, and no angle violations of >4°. The 20 lowest-energy conformers were selected for further analysis. The analysis of Ramachandran angles for the 20 lowest-energy structures was carried out using PROCHECK-NMR (*35*).

RESULTS

The primary sequences of both MSI-78 and MSI-594 are reported in Figure 1. The two peptides differ significantly at their C-termini. Figure 2 shows the alpha proton chemical shift indices for both MSI-78 and MSI-594. Both histograms indicate that the helical region extends along most of the polypeptide chains. The two profiles are very similar to those of the magainin 2 variants studied in both DPC micelles and DOPC vesicles. Figure 3 shows the summaries of the backbone NOEs found for the two peptides. The $i−i + 4$ NOE typical of the α-helical structures is present for both peptides. While MSI-78 shows a more dense distribution of $i−i + 2$ and $i−i + 3$ contacts, these NOEs are absent in MSI-594. Remarkably, the distribution of the number of NOEs per residue is quite different for the two polypeptides.
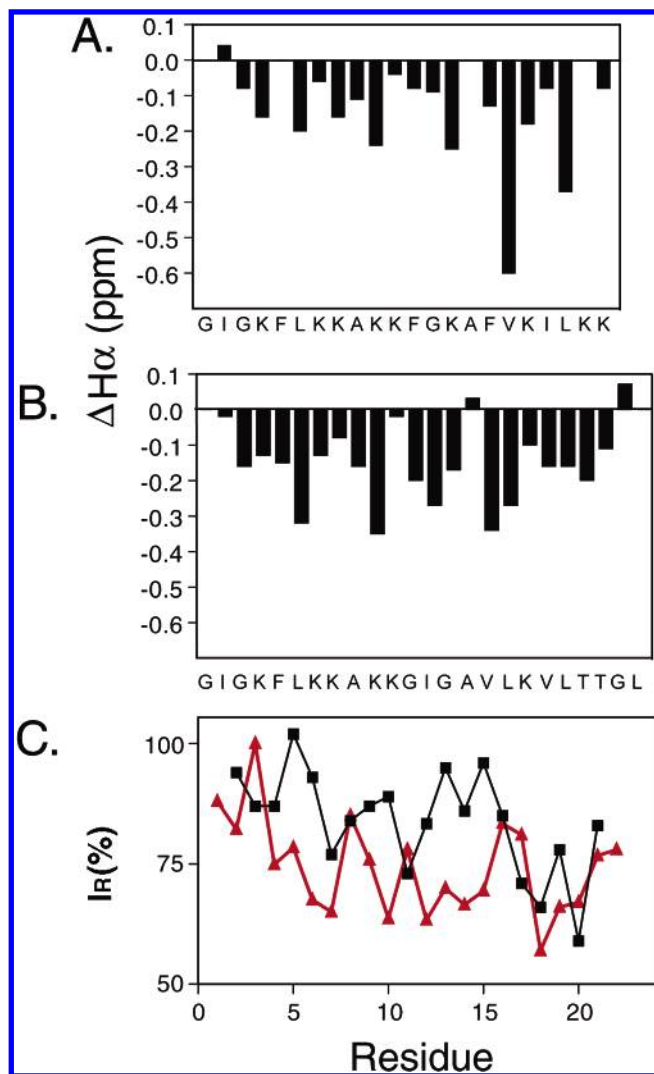
FIGURE 2: α-Proton chemical shift index for MSI-78 (A) and MSI-594 (B) solubilized in DPC micelles. (C) Intensity retention (I_R) plots of the Hα proton of MSI-78 (black trace) and MSI-594 (red trace) upon addition of 1 mM MnCl$_2$.

While MSI-78 exhibits a more uniform histogram of inter- and intraresidue NOEs, MSI-594 displays a bimodal distribution, with a low number of dipolar contacts localized around the "GIG" sequence of the molecule (Figure 4). Two slightly different structural ensembles satisfy all of the assigned NOEs from the ^{1}H$-^1$H NOESY experiments (Figure 5). One possible explanation is that the GIG sequence introduces additional dynamics in MSI-594, thereby increasing the overall backbone flexibility.

However, the network of NOE contacts for MSI-78 is denser, with seven unambiguously assigned dipolar contacts between the two protomers. As an example, Figure 6 shows a portion of the two-dimensional ^{1}H$-^1$H NOESY spectrum with the intermonomer NOEs between Phe12 and Phe16 and between Phe12 and Phe5. Similar NOEs were detected by Matsuzaki and co-workers for magainin 2 in the presence of a POPC vesicle suspension and using TRNOE at 45 °C (16). The resulting structural ensemble reported in Figure 7 shows that MSI-78 is arranged in a distorted α-helical conformation in a short coiled-coil structure with the two protomers in an antiparallel orientation. As shown in Figure 7A, the central core of the dimer is arranged with a "phenylalanine zipper" to form a hydrophobic interface to

hold the two protomers, while all the lysine residues point toward the bulk solvent. Unlike that of the conformers obtained in POPC vesicles, the packing of the phenylalanines is less defined. Since there is a slight broadening for F5, F12, and F16 in the NOESY spectra, this result is not due to calculation artifacts; rather, it reflects a possible conformational interconversion on a slow to intermediate NMR time scale.

To probe the residues of the two peptides which are solvent exposed, we added MnCl$_2$ to the NMR samples and quantified the paramagnetic line broadening of the HN$-$Hα and Hα$-$Hβ peaks in the 2D ^{1}H TOCSY experiments (36). Note that the experiments were carried out under the same experimental conditions for both peptides. The percent intensity retention plots reported in Figure 2C for the two peptides differ significantly. Upon addition of the paramagnetic ions, MSI-594 shows a decrease in the NMR signal intensities that become more pronounced and homogeneous in contrast to MSI-78, whose hydrophobic core resonances, with the exception of residues 7 and 11, are only marginally affected by the paramagnetic agent.

Magic Angle Spinning NMR Experiments. Recent CD studies carried out by Mecke and co-workers (10) show that MSI-78 is unstructured in aqueous solution, while it adopts a helical conformation upon interaction with POPC small unilamellar vesicles. These results are in agreement with the solution NMR studies, presented above, carried out in detergent micelles. Even though solution NMR experiments on DPC micelles provide high-resolution structures, the structural results obtained from a detergent micelle need to be substantiated by studies in lipid bilayers, which do not have a curved surface and are a better approximation to cell membranes. Therefore, we performed solid-state NMR experiments on both magainin analogues reconstituted in lipid bilayers. Multilamellar vesicles containing synthetic peptides selectively labeled with ^{13}C and ^{15}N isotopes were used to measure the isotropic ^{13}C chemical shift frequency. Via measurement of the deviation of the isotropic chemical shifts from the random-coil values, it is possible to infer the backbone conformation of polypeptides (37, 38). Figure 8 shows the difference between the FIDs obtained without (S_0) and with (S_1) 180° pulses in the ^{15}N channel. Both experiments were carried out with the same number of scans and a 1.6 ms REDOR dephasing time. The spectra of the peptides reconstituted in multilamellar vesicles (POPC and 3:1 POPC/POPG) containing 3 mol % MSI-78 or 3 mol % MSI-594 show that the ^{13}C-labeled site (^{13}C′-Ala) has an isotropic chemical shift value (∼176$-$178 ± 1 ppm) characteristic of residues in an α-helical conformation (39, 40). The observed line width (1$-$2 ppm) may be attributed to the backbone dynamics and/or conformational disorder of the two peptides. In the case of MSI-78, we observed narrower lines, corresponding to a less dynamic conformation, while for MSI-594, we observed broader lines, corresponding to conformational heterogeneity and dynamics. While more experiments need to be performed to reach firm conclusions, these REDOR data show that (a) both peptides adopt a helical conformation in lipid membranes and (b) MSI-78 possesses a more compact structure probably stabilized by intermonomer interactions in lipids. These results support the oligomerization of MSI-78 in lipids and further support our NMR results obtained in DPC micelles.
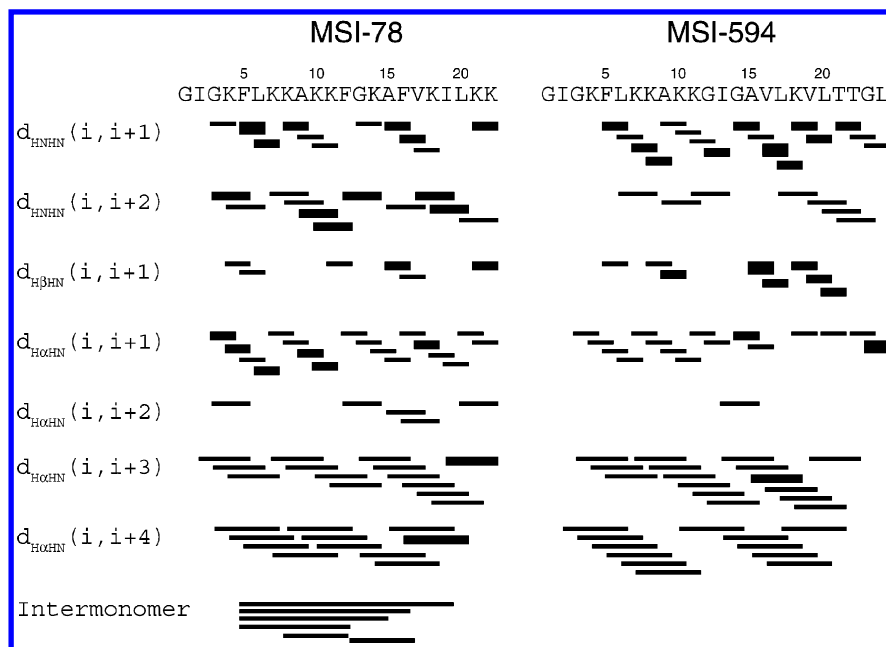
FIGURE 3: Summary of the backbone NOEs measured for MSI-78 (left) and MSI-594 (right) from $^1H-^1H$ 2D NOESY spectra acquired with a mixing time of 150 ms.
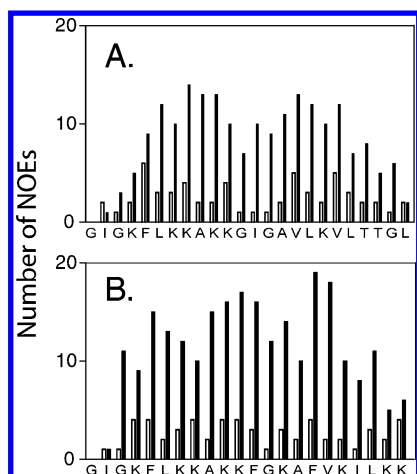

FIGURE 4: Histograms showing the intra- (black) and inter-residue (white) NOEs for both MSI-594 (A) and MSI-78 (B).
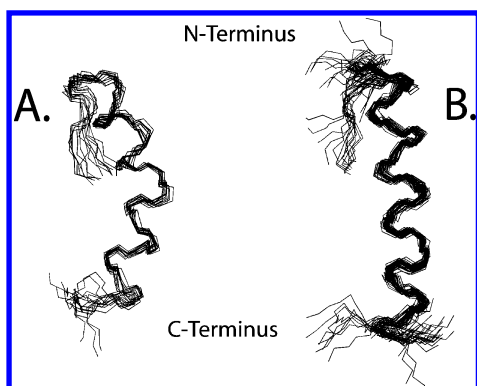

FIGURE 5: Backbone traces of MSI-594 conformers. (A) First family (15 conformers) showing a distinct kink around the GIG sequence. (B) Second family (40 conformers) showing a less pronounced kink.

DISCUSSION

To study the structures of both MSI-594 and MSI-78, we chose zwitterionic detergent micelles containing the PC
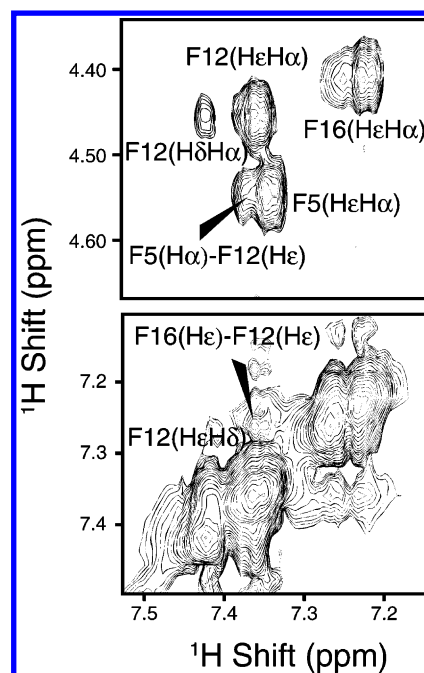

FIGURE 6: Aromatic region of the 2D $^1H-^1H$ NOESY spectra acquired with a mixing time of 150 ms, showing the intermonomer dipolar contacts between Phe12 and Phe16 and between Phe12 and Phe5.

headgroups. Under our experimental conditions, we observed the formation of antiparallel dimers only for MSI-78, while MSI-594 under the same experimental conditions or at higher peptide:detergent ratios did not dimerize. These results show that magainin aggregation is driven by the primary sequence rather than the membrane mimicking system (i.e., detergent micelles vs lipid vesicles) as previously reported. The intramonomer NOE contacts observed for MSI-78 cannot be caused by nonspecific interactions (i.e., nonspecific aggregation).

It has been demonstrated that magainin 2, a peptide similar to MSI-78, forms dimers in PC vesicles. The first evidence
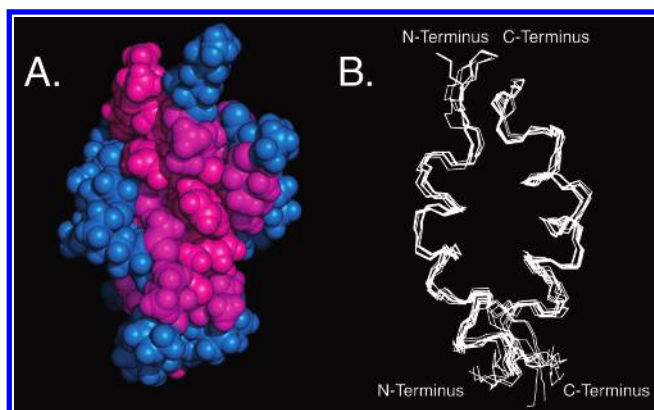
FIGURE 7: Dimeric structures of MSI-78 in DPC micelles. (A) Mapping of the hydrophilic (blue) and hydrophobic (magenta) residues onto the relaxed average structure of the MSI-78 dimer. (B) Superposition of 10 lowest-energy conformers.
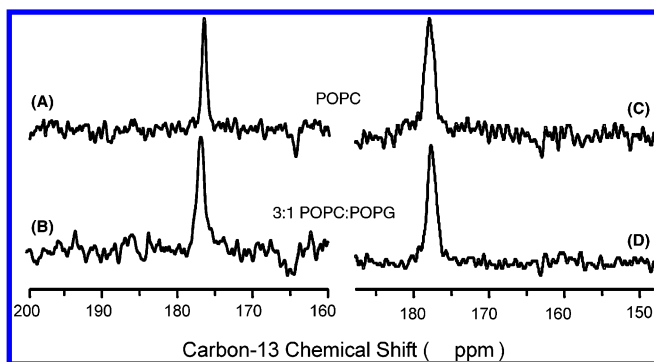

FIGURE 8: REDOR difference spectra of POPC (A and C) and 3:1 POPC/POPG (B and D) MLVs containing 3 mol % MSI-78 (A and B) and MSI-594 (C and D) at −15 °C. Approximately 32 000, 41 000, 42 000, and 43 500 scans were used to obtain spectra A−D, respectively.

came from the binding isotherms obtained in the presence of lipids containing PC headgroups (*41*). These binding curves exhibit sigmoidal behavior, indicating that intermediate oligomers such as dimers may be forming. Further proof was obtained by Matsuzaki and co-workers, who solved the structure of magainin 2 using TRNOE experiments on magainin 2 reconstituted in PC vesicles (*16*). The magainin 2 structure obtained by these authors consists of an antiparallel dimer with the two α-helices from residue 9 to 20. The overall organization of the dimer is similar to what we found for MSI-78. In the magainin 2 dimer, the aromatic residues hold together the protomers that stabilize the self-assembly of the coiled-coil structure in the absence of any ionic interactions between carboxylate groups and positively charged groups.

In DPC micelles, MSI-78 consists of an antiparallel dimer in which the two α-helices span almost the entire length of the polypeptide. This can be seen directly from the NOE summary in Figure 3, where the $i-i + 4$ contacts extend along the whole peptide backbone. A possible reason for this discrepancy is the higher sensitivity that solution NMR in micelles offers as compared to the vesicles. It is possible that the combination of dynamics and slow tumbling time of the vesicle obliterate the weak $i-i + 4$ contacts in the N-terminal portion of the peptide. Another explanation would be that the micellar environment may induce a somewhat higher helical content. Another substantial difference between the structures determined in vesicles and in micelles is the

higher density of NOE determined in the core region of magainin 2 in vesicles. This may be due to the bulkier tryptophan side chains that could pack the hydrophobic core more effectively than the phenylalanine residues present in MSI-78. As a result, the resolution of the side chains in the cores of our calculated structures is lower. This lack of resolution in the dimer core may also reflect dynamics in the slow to intermediate time scale, as manifested in the slight broadening observed for the phenylalanine peaks in the 2D spectra.

In addition to the two extra glycine and leucine residues at the C-terminus, MSI-594 presents the following mutations with respect to MSI-78: F12G, G13I, K14G, F16V, V17L, and I19V. While V17L and I19V can be considered conservative mutations, F12G, G13I, K14G, and F16V are probably responsible for the destabilization of the dimer. Given the number of dipolar contacts observed for F12 and F16, the substitution of these residues with G12 and V16 may disrupt the phenylalanine zipper that holds together the protomers in MSI-78. The GIG motif found in MSI-594 in the middle of the helix creates a substantial curvature of the polypeptide chain and probably introduces more dynamics, hampering the self-association of the peptides.

The self-association found with MSI-78 is not an unexpected result. The primary sequence of this amphipathic peptide presents the necessary requirements for the formation of oligomers, with hydrophobic residues that lead to favorable burial in the dimer formation and highly charged residues that can maximize stability by interacting with the highly polar water environment. In addition, the phenylalanine residues form a zipper with the classical knob-into-holes type of packing. The propensity to form stable phenylalanine as well leucine zippers has been extensively studied in model antimicrobial peptides (*42*).

Because of the growing emergency for antibiotic-resistant pathogenic microorganisms, structure−function studies on magainin peptides and other antimicrobial peptides are intensifying. While the correlation between the secondary structures assumed by these polypeptides and membrane activity and selectivity is becoming better and better defined, the role of self-assembly within the membrane environment remains elusive. Indeed, oligomerization plays a vital role in the activity as well as the selectivity of antimicrobial peptides. For MSI-78, dimerization screens the hydrophobic residues that are on the front line for the interaction with cell membranes, reducing the affinity for mammalian membranes which contain zwitterionic lipids in the outer leaflet. On the other hand, the MSI-78 dimer is coated with positive charges, becoming more selective toward the negatively charged bacterial membranes. Of course, the current study is incomplete. More testing under different pH and salt conditions is needed both in micelles and lipid bilayers to determine whether hydrophobicity or electrostatic interactions have the stronger effect on MSI-78 self-association.

CONCLUSIONS

In sum, we have analyzed the structures of MSI-78 and MSI-594 in DPC micelles by solution NMR spectroscopy. We found that MSI-78 forms dimers stabilized by extensive hydrophobic interactions present at the interface between the two protomers, with the charged residues occupying the outer

surface of the dimer. Under the same experimental conditions, MSI-594, a variant with F12G, G13I, K14G, F16V, V17L, and I19V mutations, is monomeric. Hydrophobic interactions are responsible for stabilizing the dimer through the formation of a phenylalanine zipper. Substituting the phenylalanine residues with glycines reduces the likelihood of self-association. The different tendencies of MSI-78 and MSI-594 to self-associate are in line with the different functions and selectivities of the two peptides. In addition, the higher potency found for MSI-78 further supports the hypothesis that dimerization is an important step in the antimicrobial activity of the magainin family.

SUPPORTING INFORMATION AVAILABLE

Structural statistics for the lowest-energy structures of MSI-594 and the MSI-78 dimer in DPC micelles. This material is available free of charge via the Internet at http://pubs.acs.org.

REFERENCES

1. Zasloff, M. (1992) Antibiotic peptides as mediators of innate immunity, *Curr. Opin. Immunol. 4*, 3−7.

2. Zasloff, M., Martin, B., and Chen, H. C. (1988) Antimicrobial activity of synthetic magainin peptides and several analogues, *Proc. Natl. Acad. Sci. U.S.A. 85*, 910−913.

3. Thennarasu, S., Lee, D. K., Poon, A., Kawulka, K. E., Vederas, J. C., and Ramamoorthy, A. (2005) Membrane permeabilization, orientation, and antimicrobial mechanism of subtilosin A, *Chem. Phys. Lipids 137*, 38−51.

4. Thennarasu, S., Lee, D. K., Tan, A., Prasad Kari, U., and Ramamoorthy, A. (2005) Antimicrobial activity and membrane selective interactions of a synthetic lipopeptide MSI-843, *Biochim. Biophys. Acta 1711*, 49−58.

5. Lamb, H. M., and Wiseman, L. R. (1998) Pexiganan acetate, *Drugs 56*, 1047−1054.

6. Fuchs, P. C., Barry, A. L., and Brown, S. D. (1998) In vitro antimicrobial activity of MSI-78, a magainin analog, *Antimicrob. Agents Chemother. 42*, 1213−1216.

7. Giacometti, A., Cirioni, O., Ghiselli, R., Orlando, F., Kamysz, W., Rocchi, M., D'Amato, G., Mocchegiani, F., Silvestri, C., Lukasiak, J., Saba, V., and Scalise, G. (2005) Effects of pexiganan alone and combined with betalactams in experimental endotoxic shock, *Peptides 26*, 207−216.

8. Giacometti, A., Cirioni, O., Kamysz, W., D'Amato, G., Silvestri, C., Licci, A., Nadolski, P., Riva, A., Lukasiak, J., and Scalise, G. (2005) In vitro activity of MSI-78 alone and in combination with antibiotics against bacteria responsible for bloodstream infections in neutropenic patients, *Int. J. Antimicrob. Agents 26*, 235−240.

9. Hallock, K. J., Lee, D. K., and Ramamoorthy, A. (2003) MSI-78, an analogue of the magainin antimicrobial peptides, disrupts lipid bilayer structure via positive curvature strain, *Biophys. J. 84*, 3052−3060.

10. Mecke, A., Lee, D. K., Ramamoorthy, A., Orr, B. G., and Banaszak Holl, M. M. (2005) Membrane Thinning Due to Antimicrobial Peptide Binding: An Atomic Force Microscopy Study of MSI-78 in Lipid Bilayers, *Biophys. J. 89*, 4043−4050.

11. Egal, M., Conrad, M., MacDonald, D. L., Maloy, W. L., Motley, M., and Genco, C. A. (1999) Antiviral effects of synthetic membrane-active peptides on herpes simplex virus, type 1, *Int. J. Antimicrob. Agents 13*, 57−60.

12. Ramamoorthy, A., Marassi, F. M., Zasloff, M., and Opella, S. J. (1995) Three-dimensional solid-state NMR spectroscopy of a peptide oriented in membrane bilayers, *J. Biomol. NMR 6*, 329−334.

13. Gesell, J., Zasloff, M., and Opella, S. J. (1997) Two-dimensional ¹H NMR experiments show that the 23-residue magainin antibiotic peptide is an α-helix in dodecylphosphocholine micelles, sodium dodecyl sulfate micelles, and trifluoroethanol/water solution, *J. Biomol. NMR 9*, 127−135.

14. Bechinger, B., Kim, Y., Chirlian, L. E., Gesell, J., Neumann, J. M., Montal, M., Tomich, J., Zasloff, M., and Opella, S. J. (1991)

15. Matsuzaki, K., Mitani, Y., Akada, K. Y., Murase, O., Yoneyama, S., Zasloff, M., and Miyajima, K. (1998) Mechanism of synergism between antimicrobial peptides magainin 2 and PGLa, *Biochemistry 37*, 15144−15153.

16. Wakamatsu, K., Takeda, A., Tachi, T., and Matsuzaki, K. (2002) Dimer structure of magainin 2 bound to phospholipid vesicles, *Biopolymers 64*, 314−327.

17. Hara, T., Kodama, H., Kondo, M., Wakamatsu, K., Takeda, A., Tachi, T., and Matsuzaki, K. (2001) Effects of peptide dimerization on pore formation: Antiparallel disulfide-dimerized magainin 2 analogue, *Biopolymers 58*, 437−446.

18. Hara, T., Mitani, Y., Tanaka, K., Uematsu, N., Takakura, A., Tachi, T., Kodama, H., Kondo, M., Mori, H., Otaka, A., Nobutaka, F., and Matsuzaki, K. (2001) Heterodimer formation between the antimicrobial peptides magainin 2 and PGLa in lipid bilayers: A cross-linking study, *Biochemistry 40*, 12395−12399.

19. Zamoon, J., Mascioni, A., Thomas, D. D., and Veglia, G. (2003) NMR Solution Structure and Topological Orientation of Monomeric Phospholamban in Dodecylphosphocholine Micelles, *Biophys. J. 85*, 2589−2598.

20. Porcelli, F., Buck, B., Lee, D. K., Hallock, K. J., Ramamoorthy, A., and Veglia, G. (2004) Structure and orientation of pardaxin determined by NMR experiments in model membranes, *J. Biol. Chem. 279*, 45815−45823.

21. Powers, J. P., Tan, A., Ramamoorthy, A., and Hancock, R. E. (2005) Solution structure and interaction of the antimicrobial polyphemusins with lipid membranes, *Biochemistry 44*, 15504−15513.

22. Opella, S. J. (1997) NMR and Membrane Proteins, *Nat. Struct. Biol. 10* (Suppl.), 845−848.

23. Gesell, J., Zasloff, M., and Opella, S. J. (1997) Two-dimensional ¹H NMR experiments show that the 23-residue magainin antibiotic peptide is an a-helix in dodecylphosphocholine micelles, sodium dodecyl sulfate micelles, and trifluoroethanol/water solution, *J. Biomol. NMR 9*, 127−135.

24. Henry, G. D., Sykes, B. D. (1994) Methods to Study Membrane Protein Structure in Solution, *Methods Enzymol. 239*, 515−535.

25. Maloy, W. L., and Kari, U. P. (1995) Structure−activity studies on magainins and other host defense peptides, *Biopolymers 37*, 105−122.

26. Delaglio, F., Grzesiek, S., Vuister, G. W., Zhu, G., Pfeifer, J., and Bax, A. (1995) NMRPipe: A Multidimensional Spectral Processing System Based on UNIX Pipes, *J. Biomol. NMR 6*, 277−293.

27. Goddard, T. D., and Kneller, D.G. (1999) *SPARKY 3*, University of California, San Francisco.

28. Bax, A., and Davis, D. G. (1985) MLEV-17 Based Two-Dimensional Homonuclear Magnetization Transfer Spectroscopy, *J. Magn. Reson. 65*, 355−360.

29. Kumar, A., Ernst, R. R., and Wuthrich, K. (1980) A Two-Dimensional Nuclear Overhauser Enhancement (2D-NOESY) Experiment for the Elucidation of Complete Proton−Proton Cross Relaxation Networks in Biological Macromolecules, *Biochem. Biophys. Res. Commun. 95*, 1−6.

30. Gullion, T., and Schaefer, J. (1989) Rotational-echo double-resonance NMR, *J. Magn. Reson. 81*, 196−200.

31. Yang, J., Parkanzky, P. D., Bodner, M. L., Duskin, C. A., and Weliky, D. P. (2002) Application of REDOR Subtraction for Filtered MAS Observation of Labeled Backbone Carbons of Membrane-Bound Fusion Peptides, *J. Magn. Reson. 159*, 101−110.

32. Bennet, A. E., Rienstra, C. M., Auger, M., Lakshmi, K. V., and Griffin, R. G. (1995) Heteronuclear Decoupling in Rotating Solids, *J. Chem. Phys. 103*, 6951−6958.

33. Schwieters, C. D., Kuszewski, J. J., Tjandra, N., and Clore, G. M. (2003) The Xplor-NIH NMR molecular structure determination package, *J. Magn. Reson. 160*, 65−73.

34. Nilges, M., Gronenborn, A. M., Brunger, A. T., and Clore, G. M. (1988) Determination of Three-Dimensional Structures of Proteins by Simulated Annealing with Interproton Distance Constraints. Application to Crambin, Potato Carboxypeptidase Inhibitor and Barley Serine Proteinase Inhibitor 2, *Protein Eng. 2*, 27−38.

35. Laskowski, R. A., Rullman, J. A. C., MacArther, M. W., Kaptein, R., and Thornton, J. M. (1998) AQUA and PROCHECK-NMR: Programs for Checking the Quality of Protein Structures Solved by NMR, *J. Biomol. NMR 8*, 477−486.

Orientations of amphipathic helical peptides in membrane bilayers determined by solid-state NMR spectroscopy, *J. Biomol. NMR 1*, 167−173.

36. Damberg, P., Jarvet, J., and Graslund, A. (2001) Micellar Systems as Solvents in Peptide and Protein Structure Determination, *Methods Enzymol. 229*, 271−285.

37. Wishart, D. S., and Sykes, B. D. (1994) Chemical Shifts as a Tool for Structure Determination, *Methods Enzymol. 239*, 363−392.

38. Wishart, D. S., Sykes, B. D., and Richards, F. M. (1991) Relationship Between Nuclear Magnetic Chemical Shift and Protein Secondary Structure, *J. Mol. Biol. 222*, 311−333.

39. Henzler-Wildman, K. A., Martinez, G. V., Brown, M. F., and Ramamoorthy, A. (2004) Perturbation of the hydrophobic core of lipid bilayers by the human antimicrobial peptide LL-37, *Biochemistry 43*, 8459−8469.

40. Henzler Wildman, K. A., Lee, D. K., and Ramamoorthy, A. (2003) Mechanism of lipid bilayer disruption by the human antimicrobial peptide, LL-37, *Biochemistry 42*, 6545−6558.

41. Matsuzaki, K. (1998) Magainins as paradigm for the mode of action of pore forming polypeptides, *Biochim. Biophys. Acta 1376*, 391−400.

42. Javadpour, M. M., and Barkley, M. D. (1997) Self-assembly of designed antimicrobial peptides in solution and micelles, *Biochemistry 36*, 9540−9549.

43. Metz, G., Wu, X., and Smith, S. O. (1994) Ramped-amplitude cross polarization in magic-angle-spinning NMR, *J. Magn. Reson., Series A, 110*, 219−227.

BI0601813